

ADVANCED ENERGY MATERIALS

Supporting Information

for *Adv. Energy Mater.*, DOI: 10.1002/aenm.201500716

Novel $\text{K}_3\text{V}_2(\text{PO}_4)_3/\text{C}$ Bundled Nanowires as Superior Sodium-Ion Battery Electrode with Ultrahigh Cycling Stability

*Xuanpeng Wang, Chaojiang Niu, Jiashen Meng, Ping Hu, Xiaoming Xu, Xiujuan Wei, Liang Zhou, * Kangning Zhao, Wen Luo, Mengyu Yan, and Liqiang Mai**

Supporting Information

Novel $K_3V_2(PO_4)_3/C$ bundled nanowires as superior sodium-ion battery electrode with ultra-high cycling stability

Xuanpeng Wang[†], Chaojiang Niu[†], Jiashen Meng[†], Ping Hu, Xiaoming Xu, Xiujuan Wei, Liang Zhou*, Kangning Zhao, Wen Luo, Mengyu Yan and Liqiang Mai*

[†]These authors contributed equally to this work.

X.P. Wang, C. J. Niu, J. S. Meng, P. Hu, X. M. Xu, X. J. Wei, K. N. Zhao, W. Luo, M.

Y. Yan, Prof. L. Zhou, Prof. L. Q. Mai

State Key Laboratory of Advanced Technology for Materials Synthesis and

Processing, Wuhan University of Technology

Wuhan 430070, China

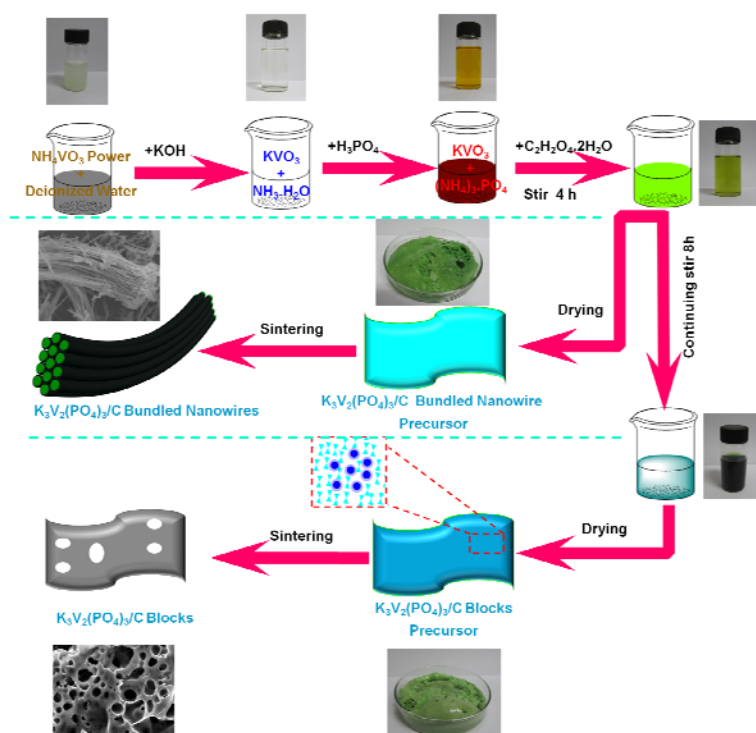


Figure S1. Schematic illustration for the fabrication process and proposed formation mechanism of the $K_3V_2(PO_4)_3/C$ bundled nanowires and blocks.

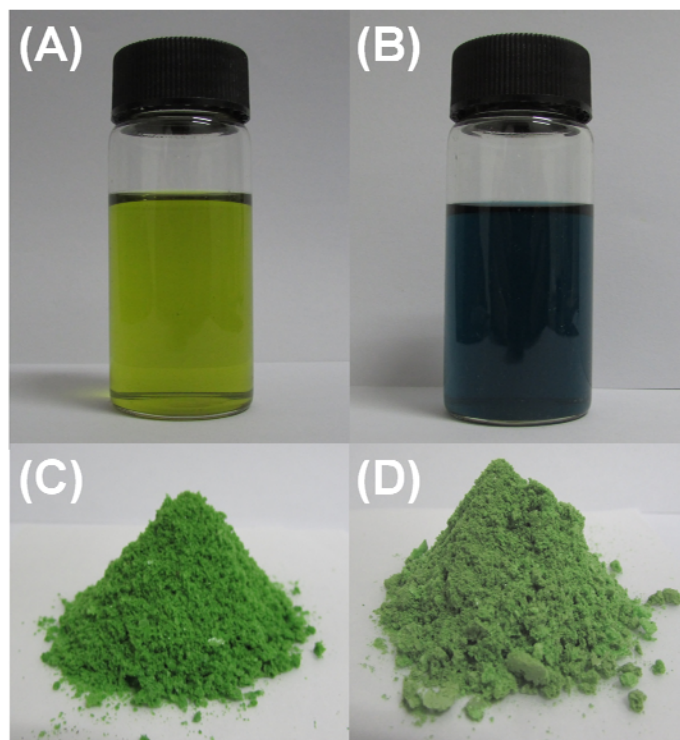


Figure S2. The photos for solution precursor of $\text{K}_3\text{V}_2(\text{PO}_4)_3$ bundled nanowires (A) and blocks (B). The photos for dried precursor of $\text{K}_3\text{V}_2(\text{PO}_4)_3$ bundled nanowires (C) and blocks (D).

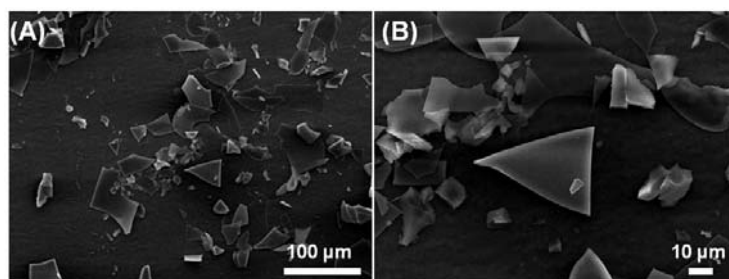


Figure S3. (A, B) SEM images of the $\text{K}_3\text{V}_2(\text{PO}_4)_3$ precursor baked at 180°C for 2h.

Table S1. The ICP test results of the $\text{K}_3\text{V}_2(\text{PO}_4)_3/\text{C}$ bundled nanowires.

Temperature	K: V: P
700 °C	3.0 : 2.04 : 2.97
800 °C	3.0 : 2.06 : 3.04
900 °C	3.0 : 1.99 : 3.08

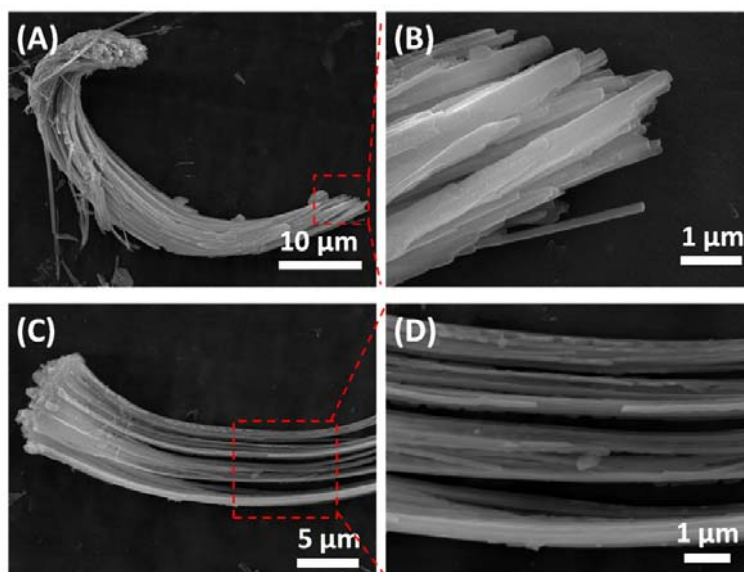


Figure S4. SEM images of the $K_3V_2(PO_4)_3/C$ bundled nanowires sintered at 800 °C.

Table S2. The ICP test results of the $K_3V_2(PO_4)_3/C$ blocks sintered at 800 °C.

	Temperature	K: V: P
Blocks	800 °C	3.00 : 2.03 : 3.01

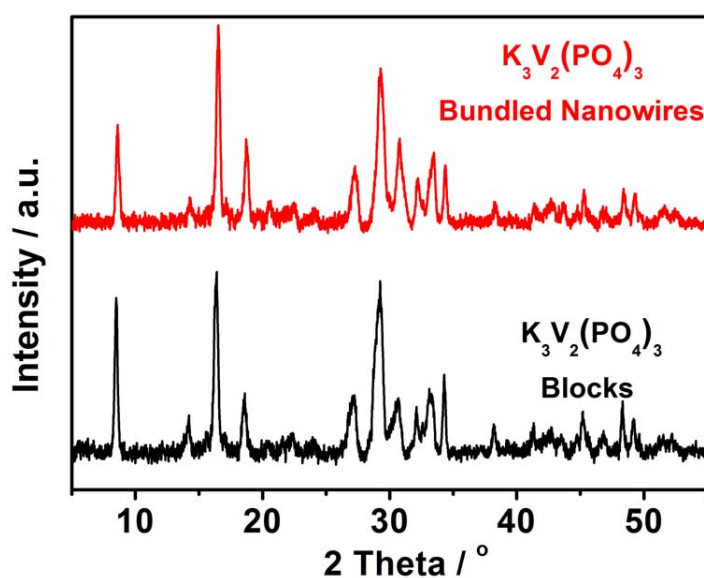


Figure S5. XRD patterns of the $K_3V_2(PO_4)_3/C$ bundled nanowires and blocks sintered at 800 °C.

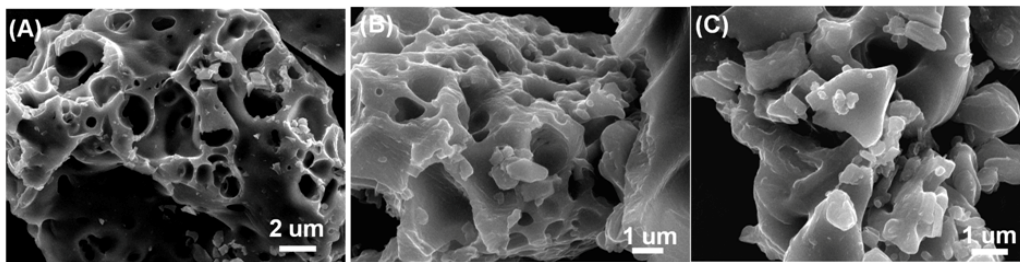


Figure S6. (A-C) SEM images of the $\text{K}_3\text{V}_2(\text{PO}_4)_3/\text{C}$ blocks sintered at 800 °C.

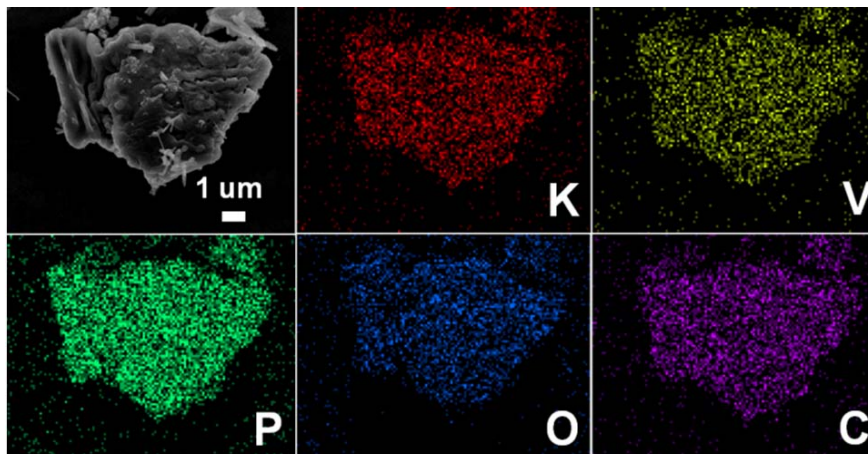


Figure S7. Elemental mapping images of the $\text{K}_3\text{V}_2(\text{PO}_4)_3/\text{C}$ blocks sintered at 800 °C.

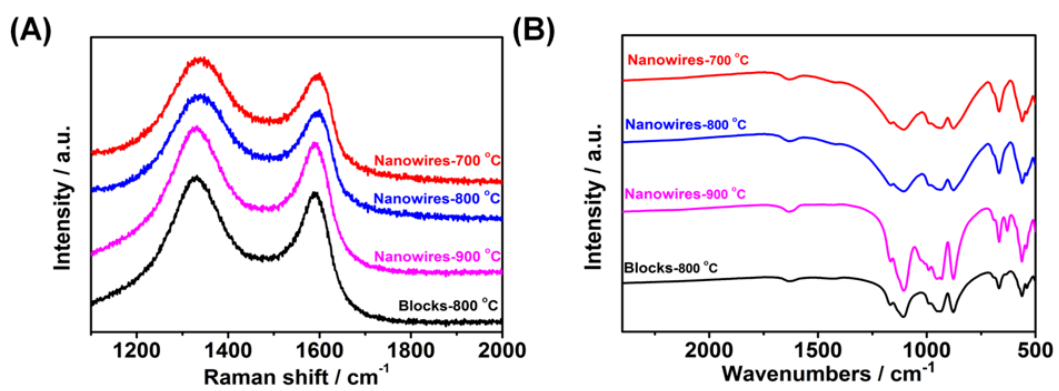


Figure S8. Raman spectra (A) and FT-IR spectra (B) of the $\text{K}_3\text{V}_2(\text{PO}_4)_3/\text{C}$ samples.

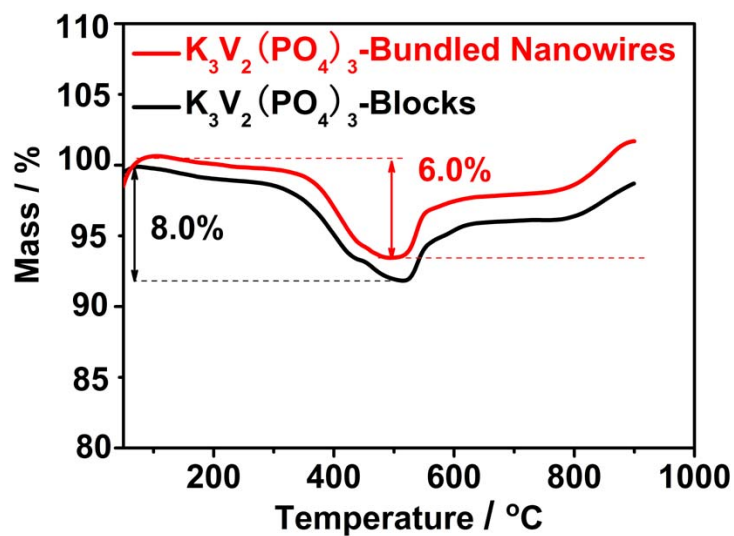


Figure S9. TGA curves of the $\text{K}_3\text{V}_2(\text{PO}_4)_3/\text{C}$ bundled nanowires and blocks sintered at 800 °C.

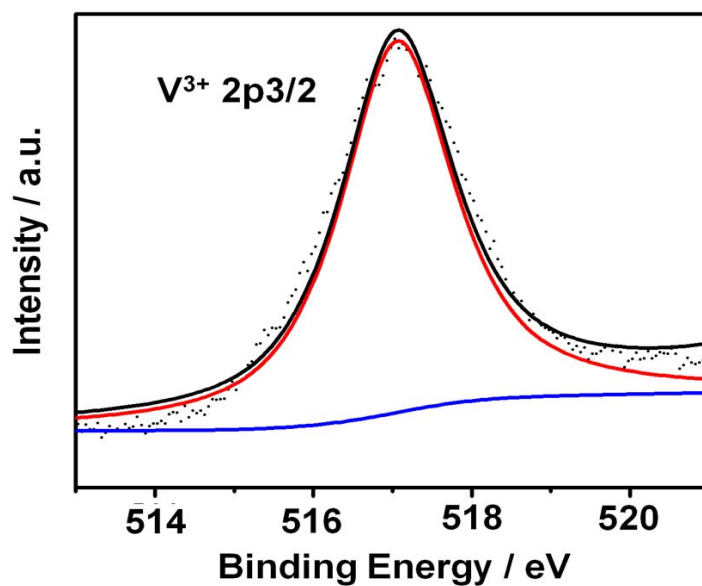


Figure S10. XPS spectra of the V $2p_{3/2}$ core level region of the $\text{K}_3\text{V}_2(\text{PO}_4)_3/\text{C}$ bundled nanowires.

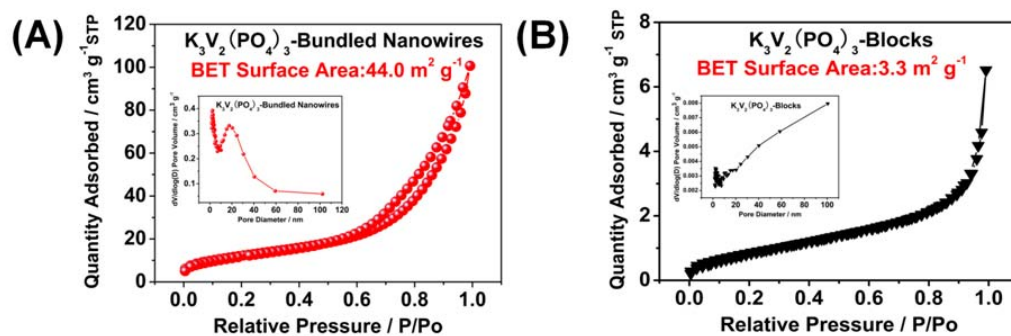


Figure S11. The nitrogen adsorption-desorption isotherms of the $K_3V_2(PO_4)_3/C$ bundled nanowires (A) and blocks (B). The pore size distribution of the $K_3V_2(PO_4)_3/C$ bundled nanowires (inset of A) and blocks (inset of B).

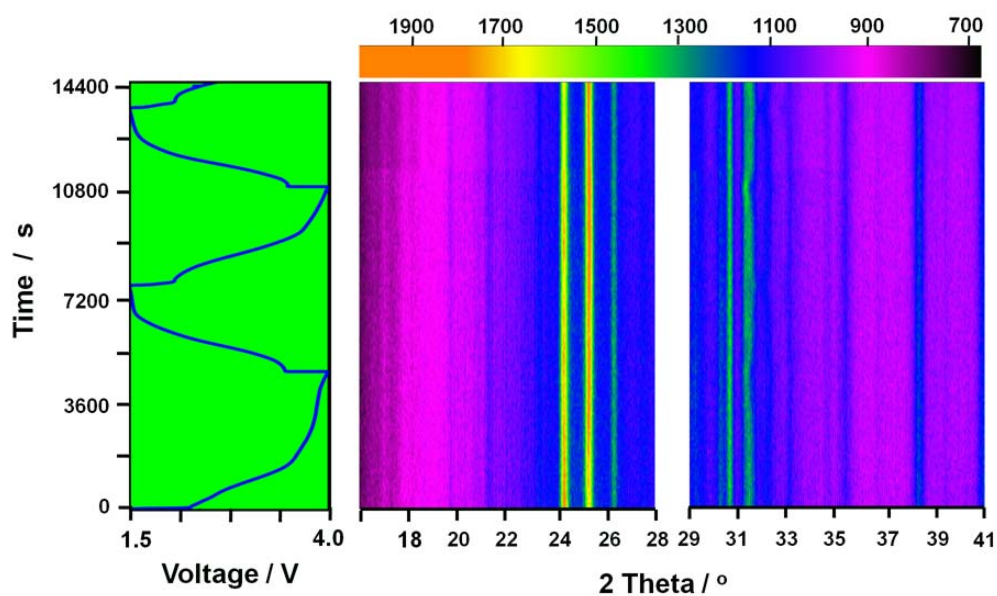


Figure S12. *In situ* X-ray diffraction patterns during galvanostatic charge and discharge of the $K_3V_2(PO_4)_3/C$ bundled nanowires at 100 mA g^{-1} .

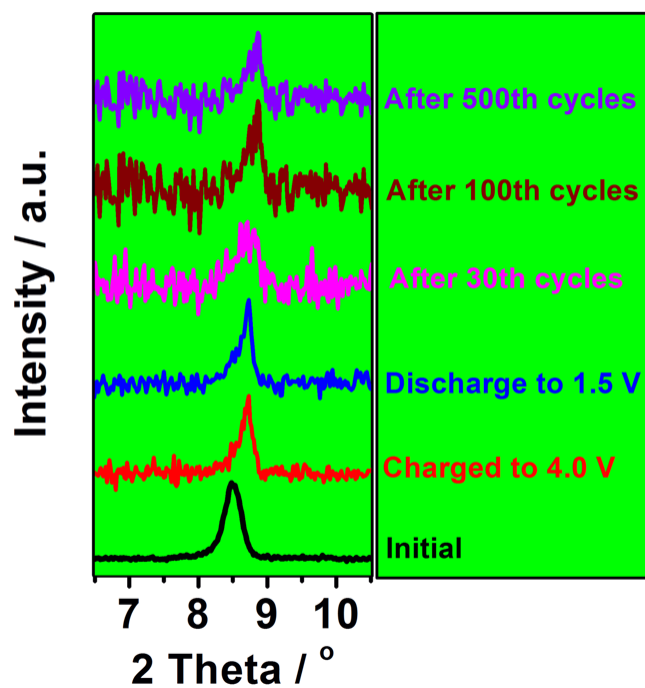


Figure S13. *Ex situ* XRD patterns of the $K_3V_2(PO_4)_3/C$ bundled nanowires.

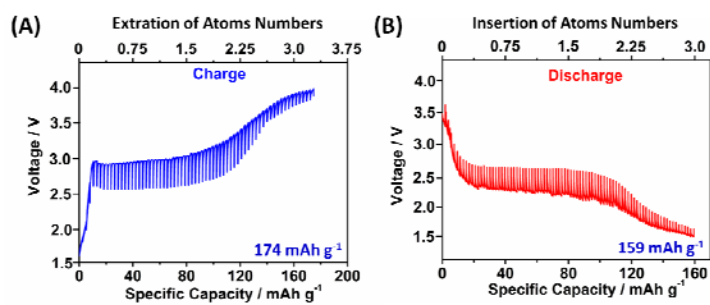


Figure S14. The galvanostatic intermittent titration technique (GITT) for $K_3V_2(PO_4)_3$ bundled nanowires.

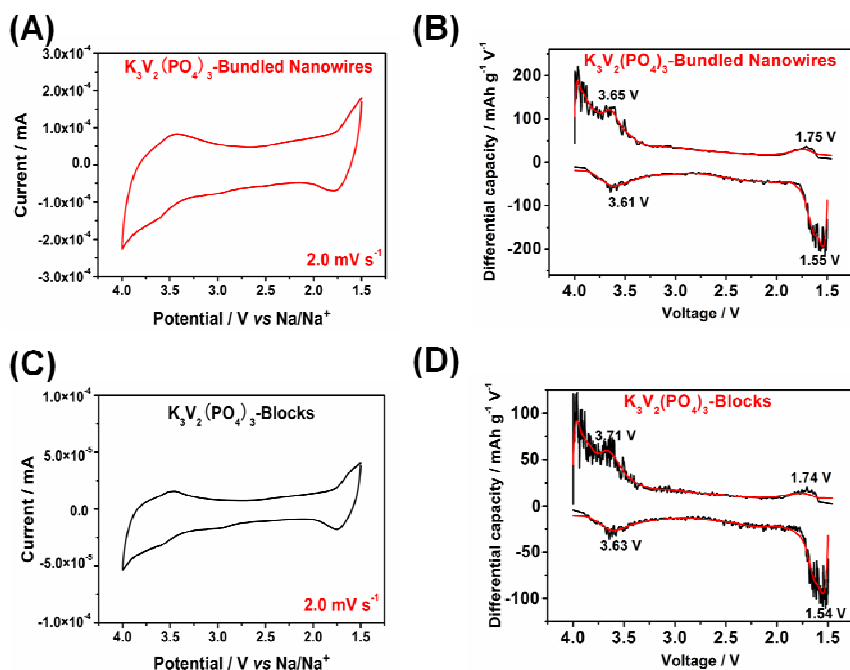


Figure S15. Cyclic voltammograms (CV) and corresponding dq/dv plots of the $K_3V_2(PO_4)_3/C$ bundled nanowires (A and B) and blocks (C and D) at a scan rate of 2.0 mV s^{-1} in the electrochemical window of 1.5 to 4.0 V vs. Na/Na^+ .

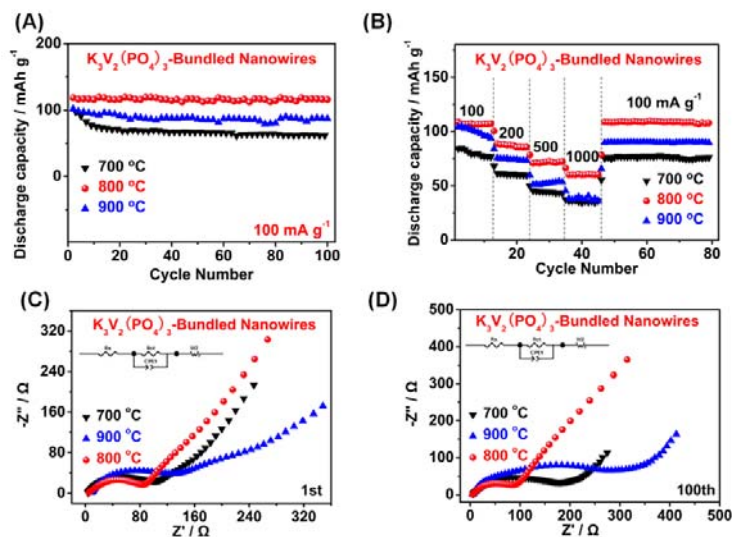


Figure S16. (A) Cycling performance of the three $K_3V_2(PO_4)_3/C$ bundled nanowires at 100 mA g^{-1} in the electrochemical window of 1.5 – 4.0 V. (B) Rate performance of the three samples. (C, D) AC impedance plots of the three samples before and after 100^{th} cycles (from 0.1Hz to 100 kHz).

Table S3. The *ex situ* ICP test results of the $K_3V_2(PO_4)_3/C$ bundled nanowires.

	K: Na: V
Before cycle	3.02 : 0.81 : 2.00
Charge to 4.0 V	1.01 : 0.01 : 2.00
Discharge to 1.5 V	1.16 : 2.10 : 2.00
After 2 cycles	1.07 : 2.26 : 2.00
After 30 cycles	1.02 : 2.25 : 2.00
After 100 cycles	1.01 : 2.24 : 2.00
After 500 cycles	1.02 : 2.25 : 2.00

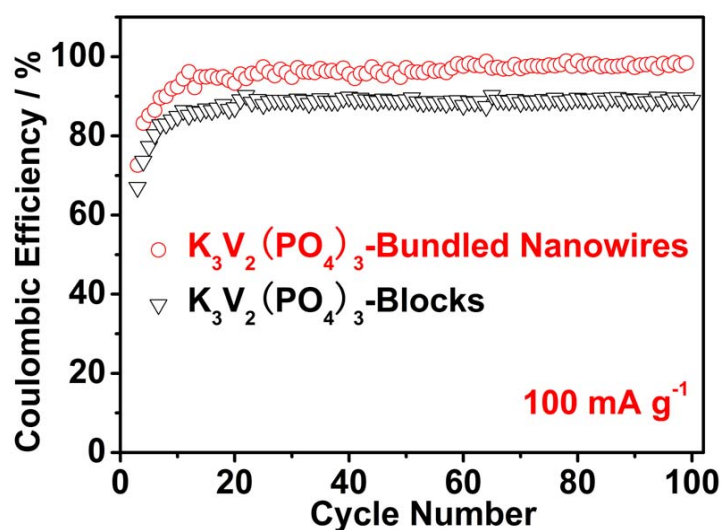


Figure S17. Coulombic efficiency of the $K_3V_2(PO_4)_3/C$ bundled nanowires and blocks at 100 mA g^{-1} .

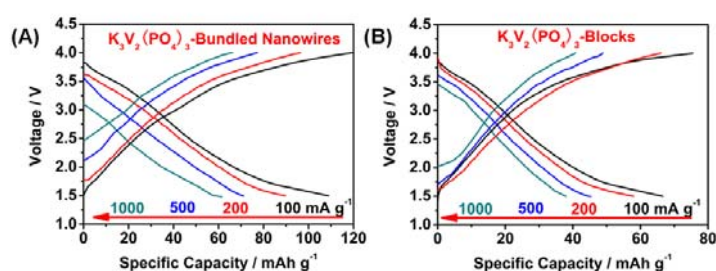


Figure S18. Charge-discharge curves of the $K_3V_2(PO_4)_3/C$ bundled nanowires (A) and blocks (B), at various current densities from 100 to $1,000 \text{ mA g}^{-1}$.

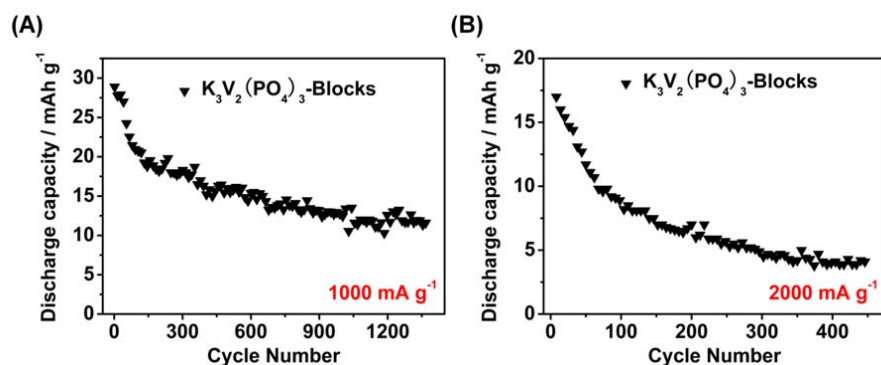


Figure S19. The cycle performances of the $\text{K}_3\text{V}_2(\text{PO}_4)_3/\text{C}$ blocks at 1,000 (A) and 2,000 mA g^{-1} (B).

Table S4. Comparison of the electrochemical performance of phosphate based electrodes for sodium-ion batteries.

	Material	Current density (mA g^{-1})	Initial capacity (mAh g^{-1})	Cycle numbers	Per cycle decay (%)	Reference
1	$\text{K}_3\text{V}_2(\text{PO}_4)_3$	100	119	100	0.0213	Our work
		500	71.0	1,000	0.0026	
		1,000	66.0	2,000	0.0023	
		2,000	45.7	2,000	0.0016	
2		588	100.6	200	0.0015	S1
3		1,176	103	1,000	0.0029	S2
4		4,700	60	30,000	0.013	S3
5	$\text{Na}_3\text{V}_2(\text{PO}_4)_3$	1,176	86	300	0.023	S4
6		11.76	109	80	0.088	S5
7		588	95	700	0.0056	S6
8		5.88	50	50	0.146	S7

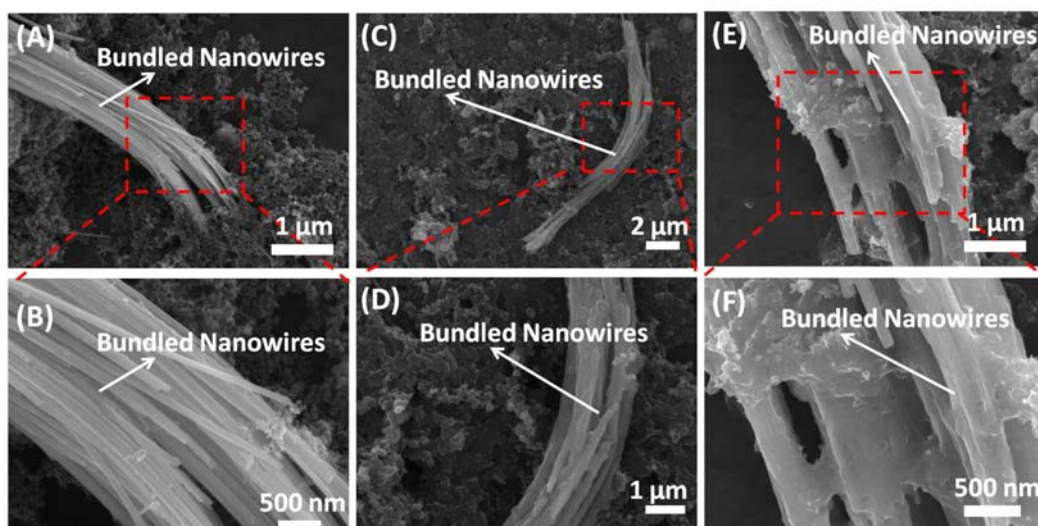


Figure S20. SEM images of the $\text{K}_3\text{V}_2(\text{PO}_4)_3/\text{C}$ bundled nanowires before cycling (A, B), after 100 cycles at 100 mA g^{-1} (C, D), and after 2,000 cycles at $1,000 \text{ mA g}^{-1}$ (E, F).

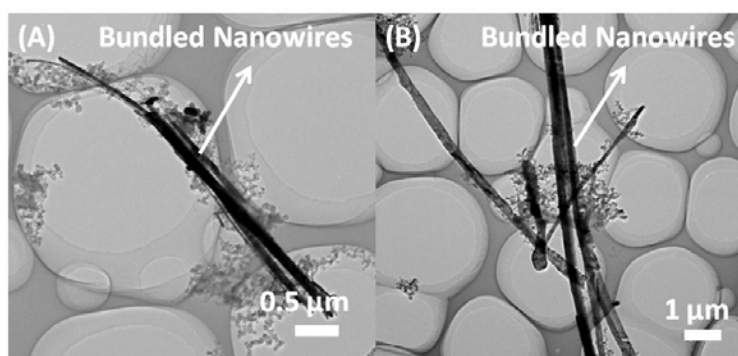


Figure S21. (A, B) TEM images of the $\text{K}_3\text{V}_2(\text{PO}_4)_3/\text{C}$ bundled nanowires after 100 cycles at 100 mA g^{-1} .

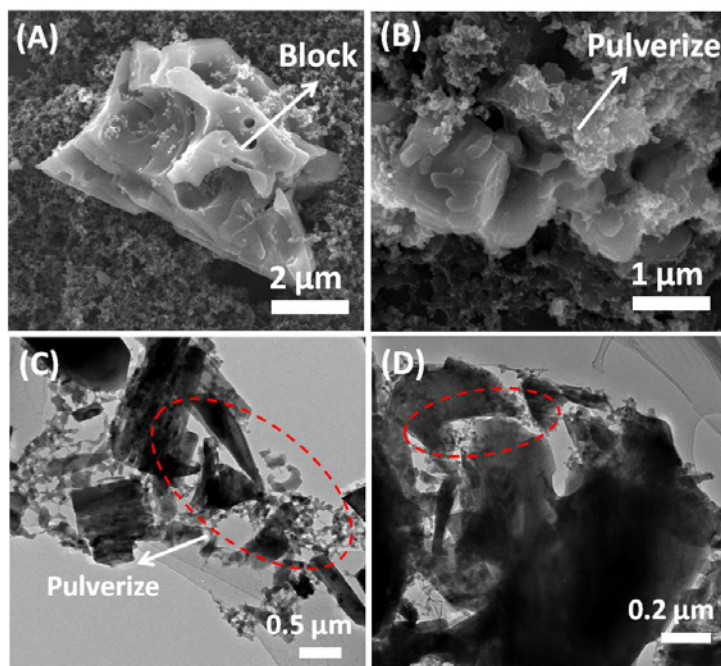


Figure S22. SEM images of the $\text{K}_3\text{V}_2(\text{PO}_4)_3/\text{C}$ blocks before cycling (A) and after 100 cycles at 100 mA g^{-1} (B). TEM images of the $\text{K}_3\text{V}_2(\text{PO}_4)_3/\text{C}$ blocks after 100 cycles at 100 mA g^{-1} (C, D).

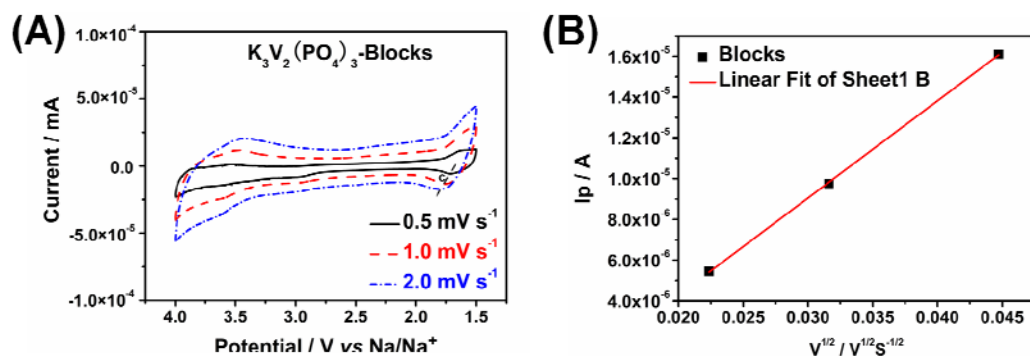


Figure S23. (A) CV curves of the $\text{K}_3\text{V}_2(\text{PO}_4)_3/\text{C}$ blocks in the electrochemical window of 1.5 – 4.0 V at different scan rates. (B) Cycling response of the $\text{K}_3\text{V}_2(\text{PO}_4)_3/\text{C}$ blocks analyzed by the Randles-Sevick equation.

Reference

- S1. S. Li, Y. F. Dong, L. Xu, X. Xu, L. He, L. Q. Mai, *Adv. Mat.* **2014**, 26, 3545.
 S2. C. B. Zhu, K. P. Song, Peter A. van Aken, J. Maier, Y. Yu, *Nano Lett.* **2014**, 14, 2175.
 S3. K. Saravanan, C. W. Mason, A. Rudola, K. H. Wong, P. Balaya, *Adv. Energy. Mater.* **2013**, 3, 444.
 S4. Y. H. Jung, C. H. Lim, D. K. Kim, *J. Mater. Chem. A* **2013**, 1, 11350.
 S5. Z. L. Jian, W. Z. Han, X. Lu, H. X. Yang, Y. S. Hu, J. Zhou, Z. B. Zhou, J. Q. Li, W. Chen, D. F. Chen, L. Q. Chen, *Adv. Energy Mater.* **2013**, 3, 156.
 S6. W. C. Duan, Z. Q. Zhu, H. Li, Z. Hu, K. Zhang, F. Y. Cheng, J. Chen, *J. Mater. Chem. A* **2014**, 2, 8668.
 S7. W. Shen, C. Wang, H. M. Liu, W. S. Yang, *Chem. -Eur. J.* **2013**, 19, 14712.